To: Dennis McGillicuddy
From: Larry Anderson
Date: October 3, 2008

North Atlantic Report #62:
Maltrud's Simulations with 3 Phyto Groups

1. The BEC Model: Phytoplankton Equations (See also Tables 1-2)

```
d[spC]/dt = photoC_sp - graze_sp - sp_loss - sp_agg
d[spChl]/dt = photoacc_sp - thetaC_sp * (graze_sp + sp_loss + sp_agg)
d[diatC]/dt = photoC_diat - graze_diat - diat_loss - diat_agg
d[diatChl]/dt = photoacc_diat - thetaC_diat * (graze_diat + diat_loss + diat_agg)
d[diazC]/dt = photoC_diaz - graze_diaz - diaz_loss
d[diazChl]/dt = photoacc_diaz - thetaC_diaz * (graze_diaz + diaz_loss)
```

common terms:

```
thetaC_sp = spChl / (spC + 1.0e-8)
thetaC_diat = diatChl / (diatC + 1.0e-8)
thetaC_diaz = diazChl / (diazC + 1.0e-8)

IF (k == 1) PAR_out = MAX(0, 0.45 * SHF_QSW)
PAR_in = PAR_out
KPARdz = (0.03e-2 * (spChl + diatChl + diazChl) + 0.04e-2) * dz(k)
PAR_out = PAR_in * EXP(-KPARdz)
PAR_avg = PAR_in * (1 - EXP(-KPARdz)) / KPARdz

Tfunc = 2.0**((TEMP-30.0)/10.0)
```

small phytoplankton growth terms:

```
VNO3_sp = (NO3/sp_kNO3)/(1+(NO3/sp_kNO3)+(NH4/sp_kNH4))
VNH4_sp = (NH4/sp_kNH4)/(1+(NO3/sp_kNO3)+(NH4/sp_kNH4))
VNtot_sp = VNO3_sp + VNH4_sp
VFeC_sp = Fe / (Fe + sp_kFe)
VPO4_sp = PO4 / (PO4 + sp_kPO4)
PCmax = PCref * Tfunc * MIN(VNtot_sp, VFeC_sp, VPO4_sp)
light_lim = 1-EXP((-alphaChl*thetaC_sp*PAR_avg)/(PCmax+epsTinv))
PCphoto_sp = PCmax * light_lim
photoC_sp = PCphoto_sp * spC

WHERE (VNtot_sp > 0)
    VNC_sp = PCphoto_sp * Q
ELSEWHERE
    VNC_sp = 0
END WHERE
WORK = alphaChl * thetaC_sp * PAR_avg
WHERE (WORK > 0)
    pChl = 2.3 * PCphoto_sp / WORK
```

```
        photoacc_sp = (pChl * VNC_sp / thetaC_sp) * spChl
    ELSEWHERE
        photoacc_sp = 0
    END WHERE
```

diatom growth terms:

```
    VNO3_diat = (NO3/diat_kNO3)/(1+(NO3/diat_kNO3)+(NH4/diat_kNH4))
    VNH4_diat = (NH4/diat_kNH4)/(1+(NO3/diat_kNO3)+(NH4/diat_kNH4))
    VNtot_diat = VNO3_diat + VNH4_diat
    VFeC_diat = Fe / (Fe + diat_kFe)
    VPO4_diat = PO4 / (PO4 + diat_kPO4)
    VSiO3_diat = SiO3 / (SiO3 + diat_kSiO3)
    PCmax = PCref * Tfunc * MIN(VNtot_diat, VFeC_diat, VSiO3_diat, VPO4_diat)
    light_lim = 1-EXP((-alphaChl*thetaC_diat*PAR_avg)/(PCmax+epsTinv))
    PCphoto_diat = PCmax * light_lim
    photoC_diat = PCphoto_diat * diatC

    WHERE (VNtot_diat > 0)
        VNC_diat = PCphoto_diat * Q
    ELSEWHERE
        VNC_diat = 0
    END WHERE
    WORK = alphaChl * thetaC_diat * PAR_avg
    WHERE (WORK > 0)
        pChl = 3.0 * PCphoto_diat / WORK
        photoacc_diat = (pChl * VNC_diat / thetaC_diat) * diatChl
    ELSEWHERE
        photoacc_diat = 0
    END WHERE
```

diazotroph growth terms:

```
    Vfec_diaz = Fe/(Fe + diaz_kFe)
    Vpo4_diaz = PO4 / (PO4 + diaz_kPO4)
    PCmax = PCrefDiaz * Tfunc * MIN(Vpo4_diaz, Vfec_diaz)
    light_lim = 1-EXP((-alphaDiaz*thetaC_diaz*PAR_avg)/(PCmax+epsTinv))
    PCphoto_diaz = PCmax * light_lim
    photoC_diaz = PCphoto_diaz * diazC

    Vnc_diaz = PCphoto_diaz * Q
    WORK = alphaDiaz * thetaC_diaz * PAR_avg
    WHERE (WORK > 0)
        pChl = 3.4 * PCphoto_diaz / WORK
        photoacc_diaz = (pChl * Vnc_diaz / thetaC_diaz) * diazChl
    ELSEWHERE
        photoacc_diaz = 0
    END WHERE
```

small phytoplankton loss terms:

```
C_loss_thres = 0.001
IF (z(k) > z1) THEN
    IF (z(k) < z2) THEN
        C_loss_thres = C_loss_thres*(z2-z(k))/(z2-z1)
    ELSE
        C_loss_thres = 0
    END IF
END IF
spC_prime = MAX(spC - C_loss_thres, 0)

sp_loss = sp_mort * spC_prime
sp_agg = MIN(0.2*dps*spC_prime, sp_mort2 * spC_prime**2)
graze_sp = z_umax_0*Tfunc*zooC*spC_prime**2/(spC_prime**2+z_grz**2)
```

diatom loss terms:

```
C_loss_thres = 0.01
IF (z(k) > z1) THEN
    IF (z(k) < z2) THEN
        C_loss_thres = C_loss_thres*(z2-z(k))/(z2-z1)
    ELSE
        C_loss_thres = 0
    END IF
END IF
diatC_prime = MAX(diatC - C_loss_thres, 0)

diat_loss = diat_mort * diatC_prime
diat_agg = MAX(0.01*dps*diatC_prime, MIN(0.2*dps*diatC_prime,diat_mort2*diatC_prime**2))
graze_diat = diat_umax_0*Tfunc*zooC*diatC_prime**2/(diatC_prime**2+0.81*z_grz**2)
```

diazotroph loss terms:

```
C_loss_diaz = 0.01
WHERE (TEMP .LT. 15.0) C_loss_diaz = 0.001
IF (z(k) > z1) THEN
    IF (z(k) < z2) THEN
        C_loss_diaz = C_loss_diaz * (z2-z(k))/(z2-z1)
    ELSE
        C_loss_diaz = 0
    END IF
END IF
diazC_prime = MAX(diazC - C_loss_diaz, 0)

diaz_loss = diaz_mort * diazC_prime
graze_diaz = diaz_umax_0*Tfunc*zooC*diazC_prime**2/(diazC_prime**2+z_grz**2)
```

Also see Tables 1 and 2.

2. Is there 18° Mode Water in the Model?

Fig. 1a shows that in Maltrud's 0.1° run there is a 15-20°C thermostad from about 60 m to $>$ 200 m depth. This is primarily 17° and 18° Mode Water (green and yellow in Fig. 1b).

- Make a movie of Fig. 1b to see where it forms?

3. Diazotrophs: Comparison with Davis & McGillicuddy (2006)

To compare with Davis & McGillicuddy (2006), a summertime (day 285) transect at 32.0°N from the model was examined. The horizontal average (Fig. 2a) shows a subsurface maximum at 70 m, while fig. 3 in Davis & McGillicuddy (2006) shows maxima at the surface and 130 m. Probably if the model nutracline were better (deeper), the subsurface maximum would be deeper, and in better agreement with the data.

Fig. 2b shows model vertically-integrated Diazotrophs as related to other variables on day 285. The relationships (binned means and standard deviations) for all 6 summer months at this latitude are shown in Fig. 3a. DIAZ are positively correlated with positive SLA (anticyclones) that are warm and salty and of low density at 70 m i.e. regular anticyclones (not MWE). This is in good agreement with Davis & McGillicuddy (2006).

- Divide DIAZ PP by DIAZ Chl to see if the high DIAZ are growing signifcantly in situ, or if they are merely being advected in horizontally. Need the horizontal advective fluxes of DIAZ to complete this comparison.

- The large-scale DIAZ distribution (Fig. 3b) shows higher DIAZ to the north of 32°N in summer. As anticyclones preferentially propogate to the SW, correlation between high DIAZ and anticyclones could be due to advection. Though does this large-scale distribution agree with observed? I.e. should DIAZ be higher to the south? See Hood, etc.

4. Phytoplankton Pigments: Model-Data Comparison

Olga Kosnyrev's 1990-2003 estimates of phytoplankton species at BATS (based on HPLC pigments and the formulae of Letelier et al., 1993, L&O, p 1420) were compared with the model functional groups (Diatoms, Diazotrophs, and Small Phytoplankton). It is unclear however if model Diazotrophs are comparable with HPLC-based Cyanobacteria or only a subset. So two estimates of data-based SP are made: one as SP = Total Chl - Diat - Cyano (i.e. considering Diazotrophs = Cyanobacteria), and one as SP_2 = Total Chl - Diat (i.e. considering Diazotrophs $\ll$ Cyanobacteria).

The BATS data (Fig. 4) show a DCM at 80 m with Total Chl dominated by SP, with DIAT making a very small contribution. Maltrud's 0.1° run (Fig. 5) has very similar Total Chl, but with different partitioning, viz. with DIAT being almost half of Total Chl and DIAZ contributing very little. Lima's 3° run (Fig. 6) is qualitatively similar to the 0.1° run, but with lower total Chl on account of lower DIAT (Fig. 6), though still not as low as observed.

Figs. 7 and 8 show the fractions, which yield the same conclusions as Figs. 4-6.

Fig. 9 shows the BATS data as a function of both depth and time, to be compared with the 0.1° run (Fig. 10) and the 3° run (Fig. 11). DIAT Chl is more temporally patchy in the data than in the models, although DIAZ Chl is in good agreement temporally though not in magnitude.

Fig. 12 plots DIAT Chl and fraction vs. Total Chl from the BATS data. The two highest Chl events are also the two highest Diatom events, with Diatom fractions of 0.5 and 0.3. Otherwise though the trends are insignificant (Fig. 13; contrast this with the model results in fig. 4b in Report #60.)

Fig. 14 shows Total Chl as a function SP and DIAT for the BATS data, 0.1° run and 3° run. In the BATS data, apart from the two high DIAT events, DIAT is low, such that Total Chl correlates with SP. In the 0.1° run DIAT and SP make more nearly equal contributions to Total Chl. The relationship in the 3° run is similar to the 0.1° run, although high Chl values are not seen (although this is monthly model output, not 5-day output.)

- Sweeney et al. (2003) and McGillicuddy et al. (2007) agree that diatoms are a very small fraction of total Chl, unlike in the model.
- So the model does not agree in some ways with the BATS data. What do then? Modify Moore's parameter values or equations? Probably best to first try to fix the physical distributions; then the large-scale distributions (using coarse resolution runs—starting from Lima's parameters); then the eddy responses.

5. Is There a Pseudo-BATS?

Fig. 15a shows all the annual NO_3 profiles from the 0.1° run in the 75-35°W 20-40°N domain. All have too high NO_3 at 200 m, and thus a higher-than-observed gradient at 100 m. The closest fit (lowest vertically-integrated difference) is from a profiles at 20.1°N; but this is too far away to serve as a pseudo-BATS (i.e. a place that has profiles like observed at BATS). A map of the Cost (Fig. 15b) shows that best agreement with BATS occur to the south and west. Thus locations west of Bermuda should best serve as a pseudo-BATS, although agreement with BATS data is still poor (e.g. the magenta profile in Fig. 15a).

6. BATS Data and 0.1° Model: Properties by Eddy Type

Correlation coefficients between various quantities from the 1988-2006 Apr-Sept BATS data were computed (Table 3). Density at 100 m showed a slight monthly trend and so was detrended. Starting from the right-side of the table, vertically-integrated PP was significantly (> 0.20) correlated with vertically-integrated Chl and the maximum Chl value; these in turn (except for v-int Chl) were correlated with NO_3 at 100 m, which was also correlated with PON flux at 150 m and density anomaly at 100 m (i.e. cyclones or MWE). PON flux at 150 m is also anticorrelated with density at 700 m (i.e. correlated with anticyclones or MWE). All this suggests PON flux correlated with MWE, although these correlation coefficients are not a clear way to get at the response to different eddy types.

A closer look at the BATS data showed trends in NO_3 (at 100 m) and DIAT in Apr-May, so the analysis period is below changed to Jun-Oct.

Table 4 breaks down the Jun-Oct BATS data into eddy types viz. positive density anomalies at 100 m are classified as C or MWE, while positive density anomalies at 700 m are classified as C or Thinnies (TH). NO_3 at 100 m is highest in MWE and lowest in AC. (The fact that NO_3 at 100 m is higher in TH than C suggests there may be errors in classification due to uncertainty in the seasonal σ_{100m} removed.) POC and PON flux at 150 m is higher in MWE than other eddy types. PP is highest in C, while Chl is highest in MWE. Growth rate (=PP/Chl) is highest in AC, due to high PP with low Chl.

Phytoplankton species are computed according to Letelier et al. (1993), where SP=Chl–DIAT–CYANO, and SP_2=Chl–DIAT (i.e. counting CYANO as SP). Because the depth of the subsurface peaks varies, vertical integrals are computed, which requires applying Letelier's formulas above 50 m. DIAT are highest in MWE, lowest in TH. CYANO is highest in C, lowest in MWE. SP is highest in C, lowest in AC; alternatively, SP_2 is highest in MWE. By percentage, DIAT are elevated in MWE, CYANO in AC, and SP in C. These results are generally consistent with Sweeney et al. (2003) and the EDDIES data, who estimated that DIAT are associated with MWE and SP with C, and Davis and McGillicuddy (2006) who found diazotrophs associated with AC. However the sensitivity of the Table 4 estimates was examined by also trying to remove interannual and seasonal trends from the BATS density and biological data, which gave different associations with eddy types. Thus there is additional uncertainty in Table 4 due to the possible existence of interannual and seasonal trends, and the error associated with estimating and removing them. In Table 4 are presented the results most consistent with Sweeney et al. (2003) and the EDDIES data, which occurs when not removing interannual trends, and not seasonal trends from the biological data, though removing the seasonal trend from σ_{100m} is clearly necessary.

- Exclude non-eddies, identified as $\delta\sigma_{700m}$ less than a threshold? Or by weighting by $\delta\sigma_{700m}$ or $\delta\sigma_{100m}$? This will also reduce sensitivity to errors in any means or trends removed. I tried this, but it did not produce results in as good agreement with Sweeney and EDDIES.

- Removing the means from Table 4, so as to examine only the anomalies (as in Table 5), causes odd interpretations in Table 4; viz. the high MWE values cause a high mean, such that the other eddy types appear lower-than-average, rather than MWE as higher-than-average. In the 1988-2006 BATS time series there is one very strong MWE with high DIAT, outside 6 std from the mean. Exclude this (and other outliers outside 3 std?) when computing the means and trends, but not from the analysis?

Table 5 shows the model results, to be compared against the BATS data (Table 4). First, model results during winter-sping (Nov-May) must be avoided, since winter convection causes blooms and species succession not related to eddies. Thus model results only between yeardays 150 and 300 (Jun-Oct) are analyzed. Also, since we have only 2 years of model output, there are not enough eddies of each type in the model timeseries at BATS (2 C, 3 MWE, 3 AC, 0 TH). Consequently to compute the statistics in Table 5, a 35-75°W longitude band at the latitude of BATS (31.7°N) is used (Fig. 16a). The seasonal cycle (and spatial trend) is removed by objectively analyzing the timeseries at each longitude by yearday with a 30-day Gaussian weight (Fig. 16b); this seasonal cycle is then subtracted to yield the anomaly "eddy" field (Fig. 17a). (Note high-frequency variations in winter appear as false eddies.) Eddies are identified as locations where the Okubo-Weiss parameter is $<$ -2e-12 s^{-2}, and classified as C, AC, MWE or TH according to relative vorticity and density anomaly at 97 m. (Vorticity is used instead of SLA because of the error in removing the seasonal signal from the latter.) Means and standard deviations of various quantities are then computed for each eddy type (Table 5). Because of multiple grid points within the same eddy, the computed standard errors ($\sigma/\sqrt{n}$) were unreasonably small; therefore standard errors were recomputed using a $\sqrt{n}$ based on an estimate of the number of eddies of each type by subsampling the domain every 200 km and 30 days (summer only).

Table 5 shows that NO_3 at 97 m is statistically significantly higher than average in MWE and C and lower than average in TH and AC. Sinking POC flux at 159 m is enhanced in MWE, similar to PON flux in BATS data (Table 4). Vertically-integrated Chl, Primary Production (PP) and Growth Rate (=PP/Chl) are all enhanced in MWE and depressed in TH, with C and AC showing no significant signal.

Examining the different phytoplankton groups, in MWE only Diatom Chl is enhanced, though PP and growth rates for all species are enhanced. In TH, Chl, PP and growth rates of all species are depressed, though the percentage of SP has increased. In AC, the percentage if DIAZ increased, but only due to a decrease in SP Chl.

- Why does Table 5 show no real association of DIAZ with AC, while Fig. 3a does? Because Fig. 3a takes into account eddy intensity? I redid Table 5 using classification based on SLA, or weighting by density at 97 m, SLA or vorticity, but none of these produced a statistically significant association of DIAZ with AC. So is it due to the slight difference in latitude (30 vs. 31.7°N)? Otherwise it must be due to the fact that most points in Fig. 3a have low SLA.

- Future eddy-resolving simulations will need to be 10-20 years long, so that eddy statistics at e.g. BATS can be computed, to estimate the effect of different eddy types on biology.

Table 1: BEC Model Parameters

Parameter	Value	Description
alphaChl	0.25 * dps	Chl-specific initial slope of P-I curve (mmol C m^2/(mg Chl W sec))
alphaDiaz	0.028 * dps	chl. spec. init. slope of P-I curve for diazotrophs
diat_kFe	0.16e-3	diatom iron uptake half saturation coefficient (nmol Fe/m3)
diat_kNH4	0.08	diatom ammonium uptake half saturation coeff. (mmol N/m3)
diat_kNO3	2.5	diatom nitrate uptake half saturation coeff. (mmol N/m3)
diat_kPO4	0.005	diatom PO4 uptate (mmol P/m^3)
diat_kSiO3	1.0	diatom si uptake half saturation coefficient (mmol SiO3/m3)
diat_mort	0.1 * dps	diatom non-grazing death rate (1/sec)
diat_mort2	0.009 * dps	diatom quad mort rate, agg/sinking (1/sec/((mmol C/m3))
diat_umax_0	2.0 * dps	max. zoopl growth rate on diatoms at tref (1/sec)
diaz_kFe	0.1e-3	diazotroph half-saturation const. for P uptake
diaz_kPO4	0.0075	diazotroph half-saturation const. for P uptake
diaz_mort	0.18 * dps	diazotroph non-grazing death rate (1/sec)
diaz_umax_0	1.2 * dps	max. zoopl growth rate on diazotrophs at tref (1/sec)
dps	1.0/86400.0	number of days in a second
epsTinv	3.17e-8	small inverse time scale (1/year) (1/sec)
PCref	3.0 * dps	max phyto C-specific growth rate at tref (GD98) (1/sec)
PCrefDiaz	0.4 * dps	max Diaz C-specific growth rate at tref (GD98) (1/sec)
Q	0.137	constant N:C ratio = 16/117
sp_kFe	0.06e-3	small phyto iron uptake half saturation coefficient (nmol Fe/m3)
sp_kNH4	0.005	small phyto ammonium uptake half saturation coeff. (mmol N/m3)
sp_kNO3	0.5	small phyto nitrate uptake half saturation coeff. (mmol N/m3)
sp_kPO4	0.0003125	small phyto PO4 uptake (mmol P/m^3)
sp_mort	0.1 * dps	small phyto non-grazing death rate (1/sec)
sp_mort2	0.009 * dps	small phyto quad mort rate, agg (1/sec/((mmol C/m3))
z1	100.0e2	phyto loss threshold is constant for z shallower than z1 (cm)
z2	200.0e2	phyto loss threshold is zero for z deeper than z2 (cm)
z_grz	1.05	grazing coefficient for small phyto (mmol C/m^3)
z_umax_0	2.75 * dps	max. zoopl growth rate on sphyto at tref (1/sec)

Table 2: BEC Model Variables

Variable	Description
diatC	diatom carbon
diatChl	diatom chlorophyll
diazC	diazotroph carbon
diazChl	diazotroph Chlorophyll
dz(k)	level thickness (cm)
Fe	dissolved inorganic iron
k	level
NH4	dissolved ammonia
NO3	dissolved inorganic nitrate
PO4	dissolved inorganic phosphate
SHF_QSW	penetrative solar heat flux (W/m^2)
SiO3	dissolved inorganic silicate
spC	small phytoplankton carbon
spChl	small phytoplankton chlorophyll
TEMP	potential temperature (C)
z(k)	depth (cm)
zooC	zooplankton carbon

Table 3: Apr-Sept 1988-2006 BATS Data: Correlation Coefficients

	σ_{700m}	$\delta\sigma_{100m}$	NO_3	SiO_3	POC	PON	PP	v-int Chl
$\delta\sigma_{100m}$	0.243							
NO_3(100 m)	-0.080	**0.232**						
SiO_3(100 m)	0.087	0.245	0.304					
POC Flux(150 m)	-0.157	-0.091	0.196	0.050				
PON Flux(150 m)	**-0.233**	-0.054	**0.208**	-0.003	0.912			
PP, v-int	-0.135	0.044	**0.266**	-0.064	0.173	0.194		
Chl, v-int	-0.032	0.027	-0.075	-0.087	0.084	0.150	**0.297**	
Chl, max	0.075	0.116	**0.329**	0.034	0.006	0.018	**0.273**	0.722

Boldface is used for key values >0.20.

Table 4: Jun-Oct 1988-2006 BATS data: Means and Standard Errors by Eddy Type

	C	AC	MWE	TH
number of eddies	25	22	21	12
NO_3 (100 m, μM)	0.306 ± 0.074	*0.209 ± 0.099*	**0.433 ± 0.107**	0.331 ± 0.172
SiO_3 (100 m, μM)	0.750 ± 0.042	*0.541 ± 0.080*	0.754 ± 0.071	0.703 ± 0.057
POC Flux (150 m)	*21.28 ± 1.79*	23.77 ± 1.64	**24.68 ± 1.76**	22.24 ± 2.10
PON Flux (150 m)	3.36 ± 0.29	3.70 ± 0.34	**4.07 ± 0.28**	3.62 ± 0.35
PP (mg C/m^2/d)	**443 ± 27**	431 ± 26	405 ± 32	396 ± 41
Chl (mg Chl/m^2)	22.60 ± 1.17	21.29 ± 2.06	**24.04 ± 1.82**	21.95 ± 1.43
Chl, max (ng/L)	322 ± 17	297 ± 31	**369 ± 34**	317 ± 22
Growth rate (gC/gChl/d)	20.4 ± 1.7	**27.3 ± 4.4**	18.0 ± 1.4	18.2 ± 2.2
DIAT (mg Chl/m^2)	0.370 ± 0.051	0.428 ± 0.092	**1.078 ± 0.729**	*0.277 ± 0.021*
DIAT, max (ng Chl/L)	5.254 ± 0.881	6.631 ± 1.574	**26.257 ± 20.746**	5.109 ± 1.361
CYANO (mg Chl/m^2)	8.51 ± 1.67	8.61 ± 1.29	*5.82 ± 0.97*	8.63 ± 1.12
CYANO, max (ng Chl/L)	**169 ± 37**	134 ± 23	*97 ± 17*	125 ± 19
SP (mg Chl/m^2)	**19.08 ± 1.16**	*14.69 ± 1.61*	17.21 ± 1.21	16.84 ± 0.54
SP, max (ng Chl/L)	**327 ± 24**	*222 ± 21*	266 ± 20	314 ± 24
SP_2 (mg Chl/m^2)	22.63 ± 1.17	22.44 ± 1.93	23.58 ± 1.07	23.24 ± 1.28
SP_2, max (ng Chl/L)	328 ± 18	317 ± 29	**355 ± 20**	326 ± 24
Percent DIAT	1.83 ± 0.36	1.95 ± 0.39	**2.84 ± 1.39**	*1.23 ± 0.16*
Percent CYANO	31.1 ± 6.0	**41.1 ± 5.6**	*21.9 ± 3.4*	33.7 ± 3.1
Percent SP	**76.0 ± 6.4**	62.5 ± 4.4	**74.0 ± 5.7**	65.1 ± 3.4
Percent SP_2	98.6 ± 0.2	98.1 ± 0.3	97.0 ± 1.5	98.5 ± 0.3

Boldface is used for values higher than average.

Italics is used for values lower than average.

Table 5: 0.1° Model: Mean Anomalies and Standard Errors by Eddy Type

	C	AC	MWE	TH
number of grid points	1968	1514	1488	1930
approx. number of eddies	16	10	12	20
NO_3(97 m, μM)	**0.34 ± 0.17**	*-0.28 ± 0.21*	**0.86 ± 0.20**	*-1.43 ± 0.21*
SiO_3(97 m, μM)	0.00 ± 0.11	-0.03 ± 0.14	**0.53 ± 0.14**	*-0.76 ± 0.10*
POC Flux(159 m)	0.02 ± 0.10	-0.10 ± 0.16	**0.38 ± 0.14**	0.01 ± 0.11
Chl Total, v-int (mgChl/m^2)	0.15 ± 0.30	-0.32 ± 0.48	**1.09 ± 0.38**	*-1.89 ± 0.32*
PP Total, v-int (mgC/m^2/d)	2 ± 10	-9 ± 18	**38 ± 14**	*-69 ± 12*
Growth rate (g C/g Chl/d)	0.1 ± 0.3	-0.2 ± 0.6	**0.9 ± 0.4**	*-1.7 ± 0.3*
Chl Total, v-int (mgChl/m^2)	0.15 ± 0.30	-0.32 ± 0.48	**1.09 ± 0.38**	*-1.89 ± 0.32*
Chl DIAT, v-int	0.08 ± 0.25	-0.15 ± 0.41	**1.19 ± 0.34**	*-1.68 ± 0.26*
Chl SP, v-int	0.07 ± 0.10	*-0.17 ± 0.13*	-0.09 ± 0.12	*-0.20 ± 0.10*
Chl DIAZ, v-int	-0.005 ± 0.007	0.006 ± 0.013	-0.002 ± 0.008	*-0.008 ± 0.005*
Percent Chl DIAT	0.3 ± 0.7	-0.2 ± 1.2	**3.6 ± 0.8**	*-4.8 ± 0.8*
Percent Chl SP	-0.3 ± 0.7	0.1 ± 1.2	*-3.4 ± 0.8*	**4.6 ± 0.8**
Percent Chl DIAZ	*-0.06 ± 0.03*	**0.08 ± 0.06**	*-0.15 ± 0.05*	**0.22 ± 0.04**
PP Total, v-int (mgC/m^2/d)	2 ± 10	-9 ± 18	**38 ± 14**	*-69 ± 12*
PP DIAT, v-int	-1 ± 4	-2 ± 7	**22 ± 7**	*-30 ± 5*
PP SP, v-int	3 ± 7	-7 ± 11	**16 ± 8**	*-38 ± 7*
PP DIAZ, v-int	-0.03 ± 0.04	0.05 ± 0.12	**0.09 ± 0.06**	*-0.17 ± 0.03*
Percent PP DIAT	-0.1 ± 0.7	0.0 ± 1.1	**3.4 ± 0.8**	*-4.6 ± 0.7*
Percent PP SP	0.1 ± 0.7	0.0 ± 1.1	*-3.4 ± 0.8*	**4.6 ± 0.7**
Percent PP DIAZ	-0.006 ± 0.010	0.014 ± 0.026	0.011 ± 0.012	*-0.023 ± 0.006*
Growth rate (g C/g Chl/d)	0.1 ± 0.3	-0.2 ± 0.6	**0.9 ± 0.4**	*-1.7 ± 0.3*
Growth rate DIAT	0.0 ± 0.3	-0.1 ± 0.4	**1.1 ± 0.3**	*-1.8 ± 0.3*
Growth rate SP	0.2 ± 0.5	-0.3 ± 0.9	**1.9 ± 0.7**	*-3.2 ± 0.6*
Growth rate DIAZ	-0.04 ± 0.08	0.05 ± 0.18	**0.20 ± 0.11**	*-0.34 ± 0.06*

Boldface is used for values statistically higher than average.
Italics is used for values statistically lower than average.

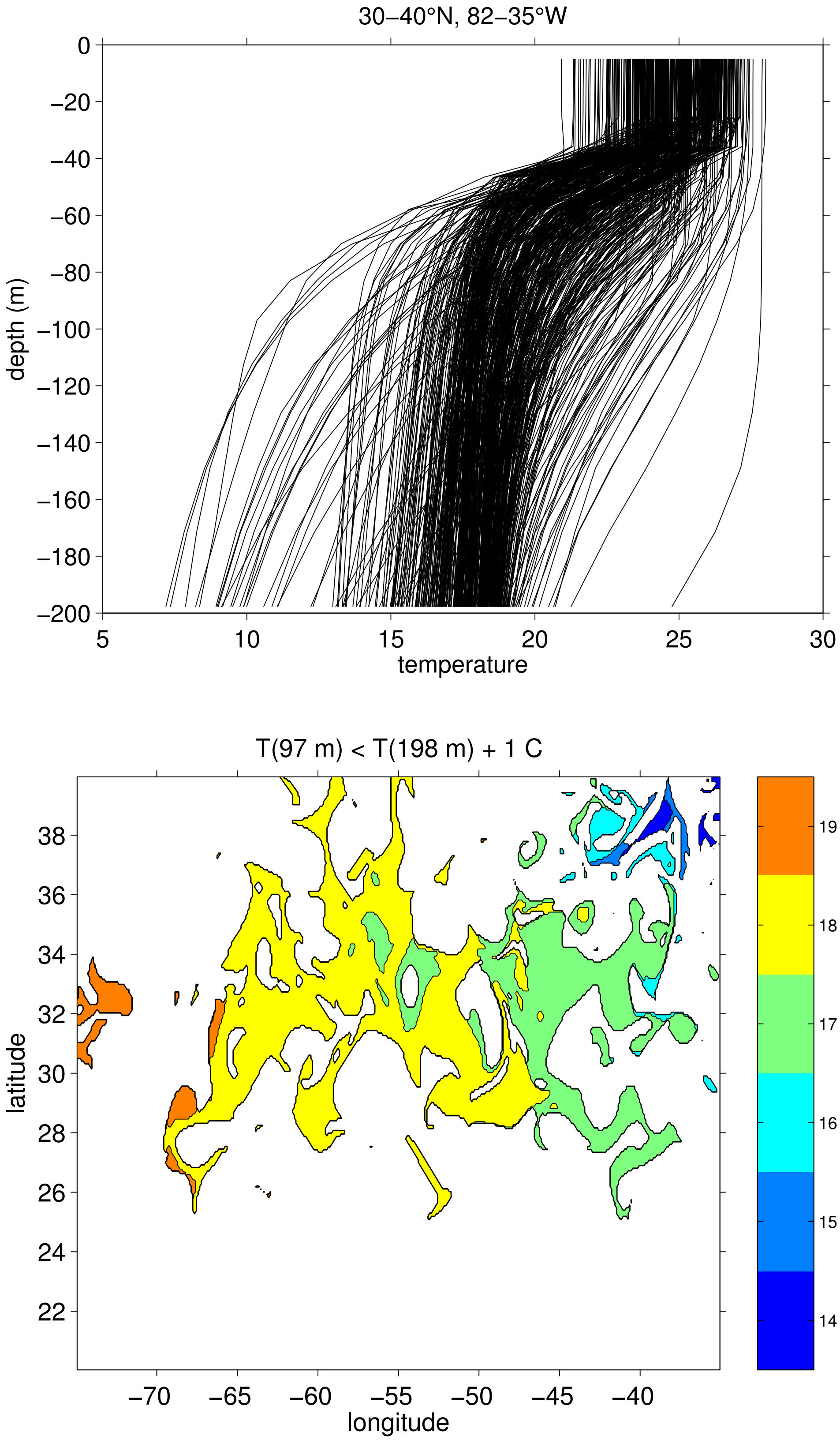

Fig. 1. Maltrud 0.1° run, Day 281-285 (Oct 8-12?).

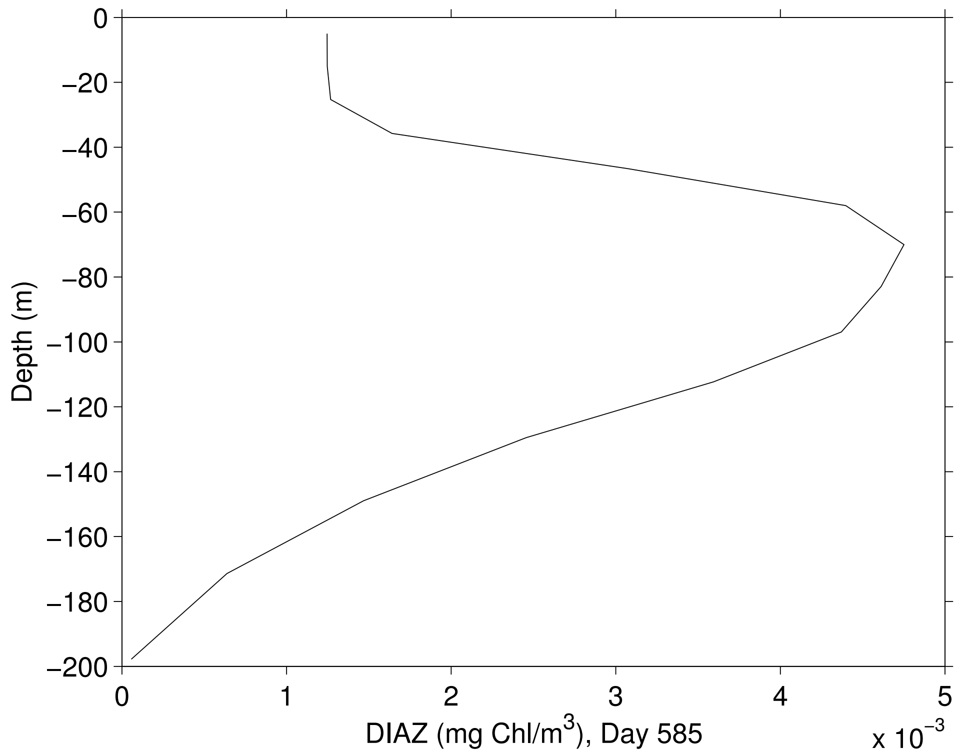

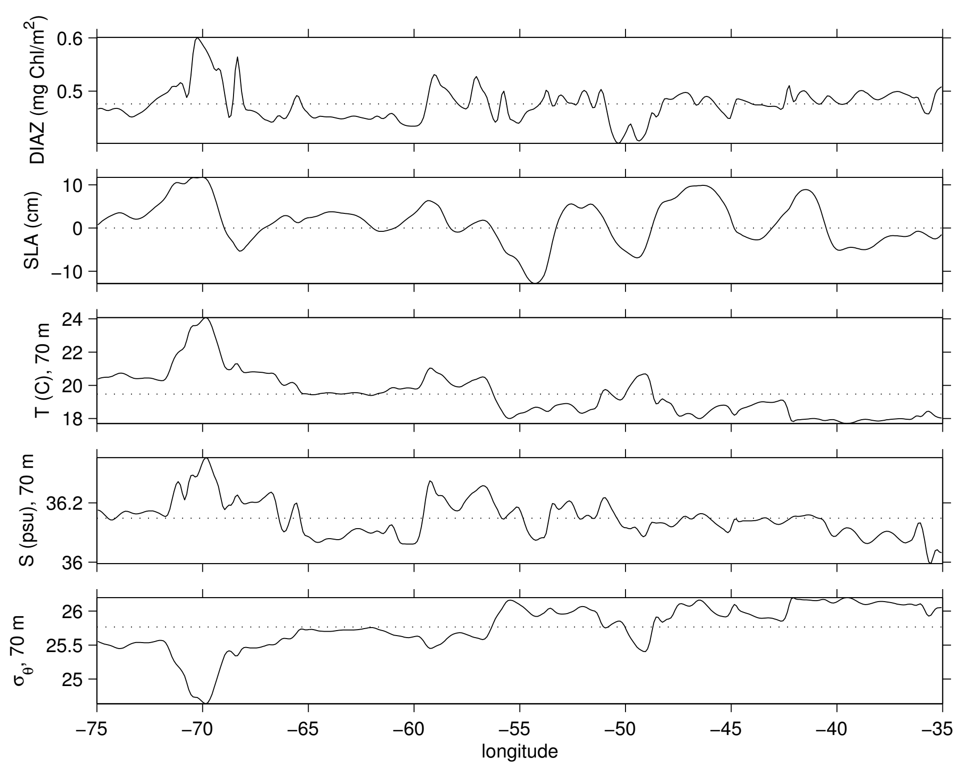

Fig. 2. (a) horizontal average at 32.0°N on Day 285.
(b) Transects on Day 285.

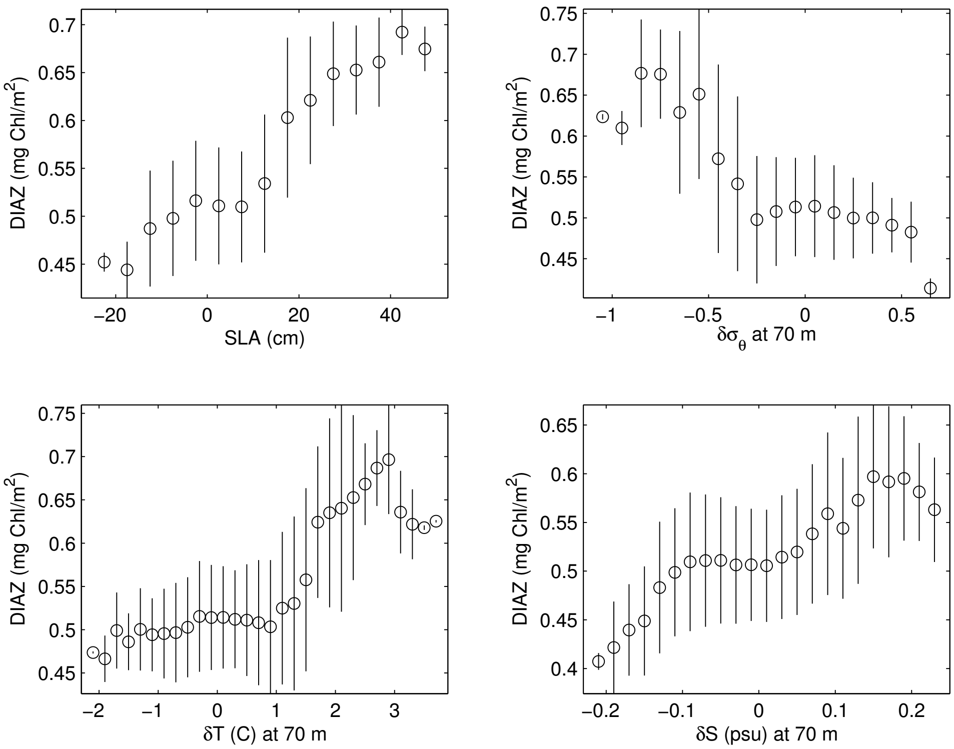

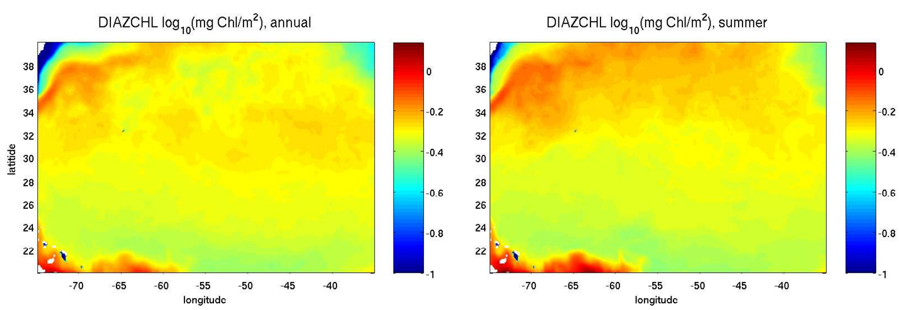

Fig. 3. (a) data from 6 summer months, years 1 & 2. (b) time-averages.

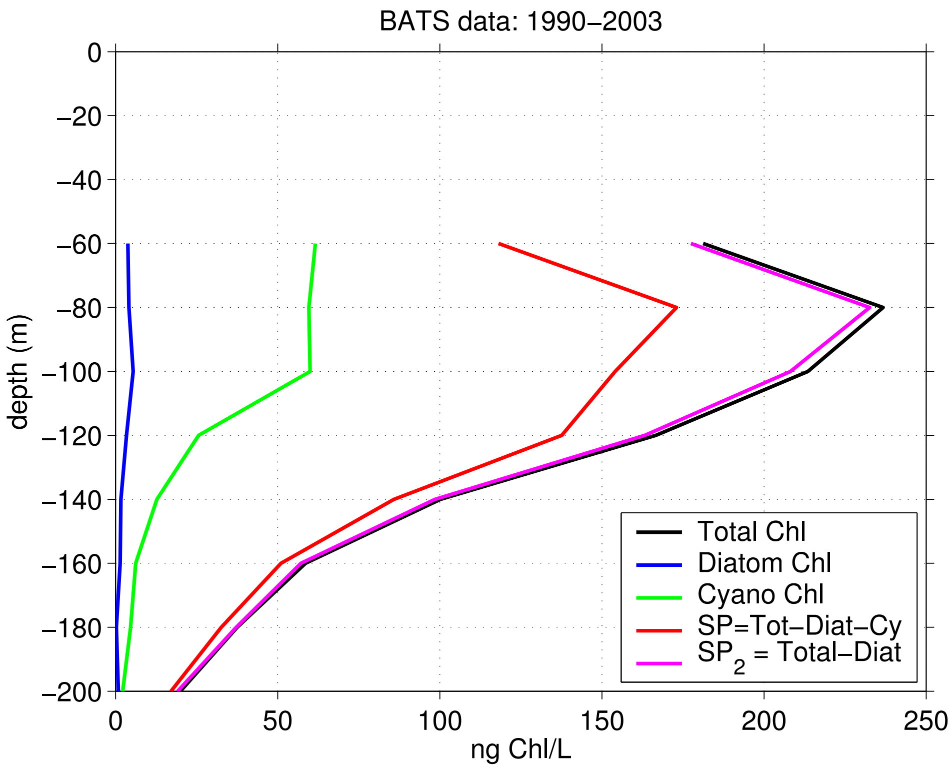

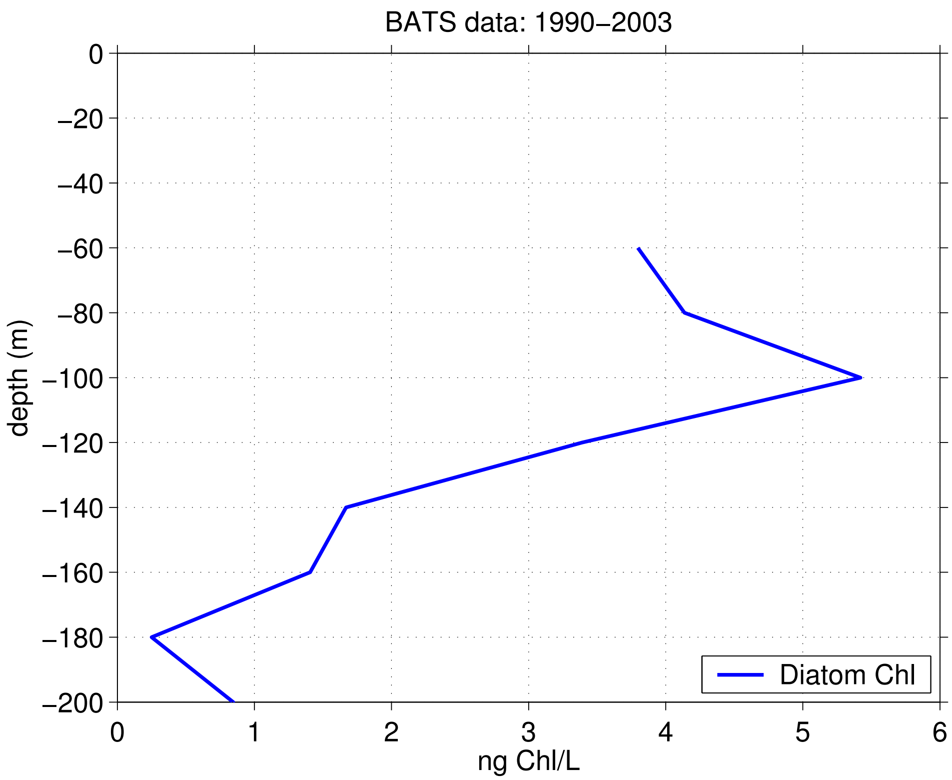

Fig. 4. BATS data.

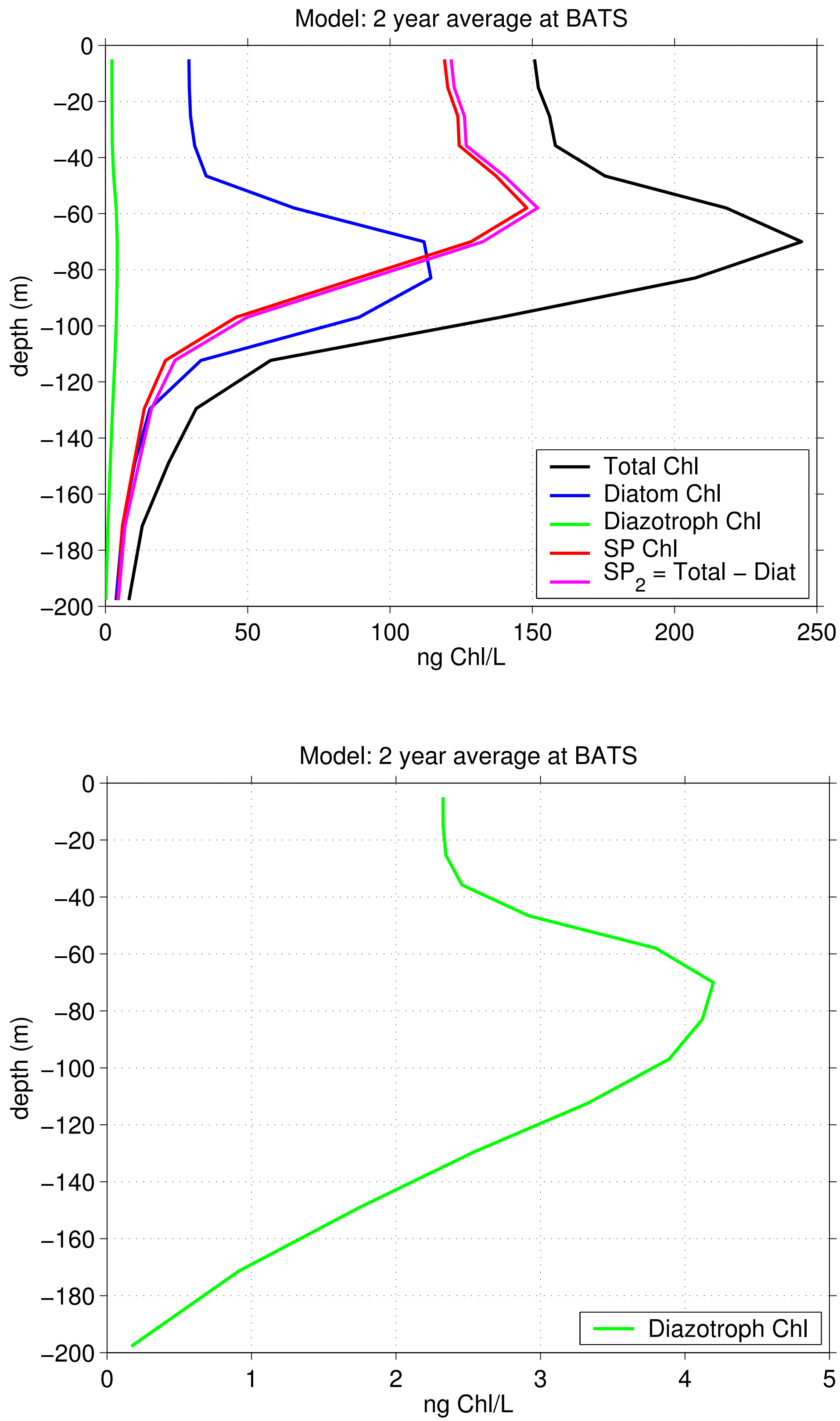

Fig. 5. Maltrud 0.1° run.

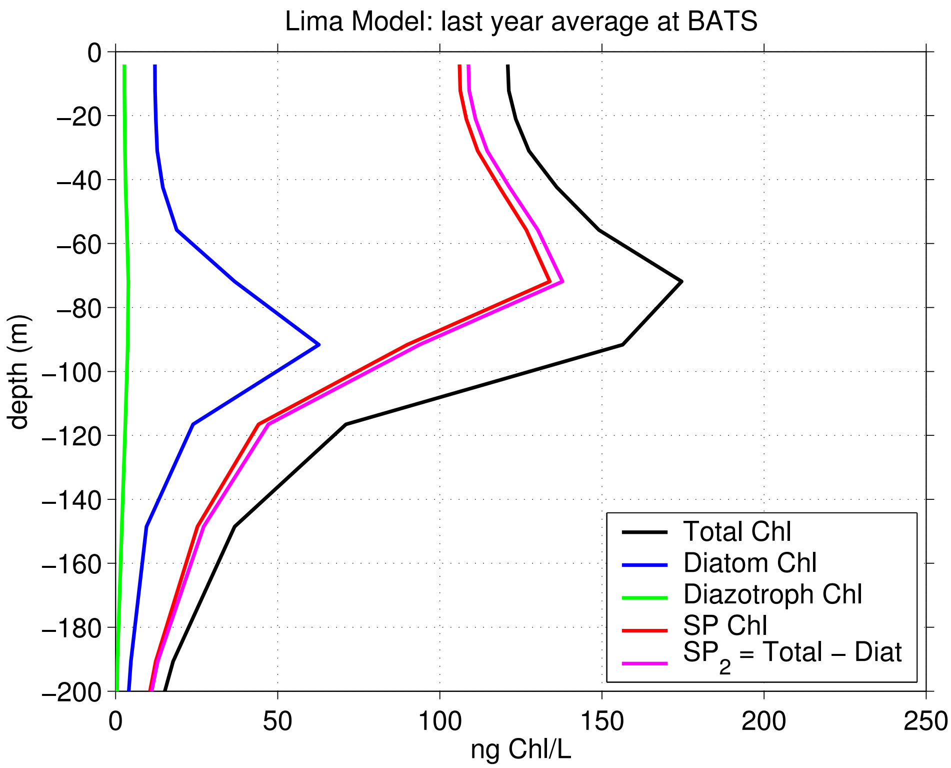

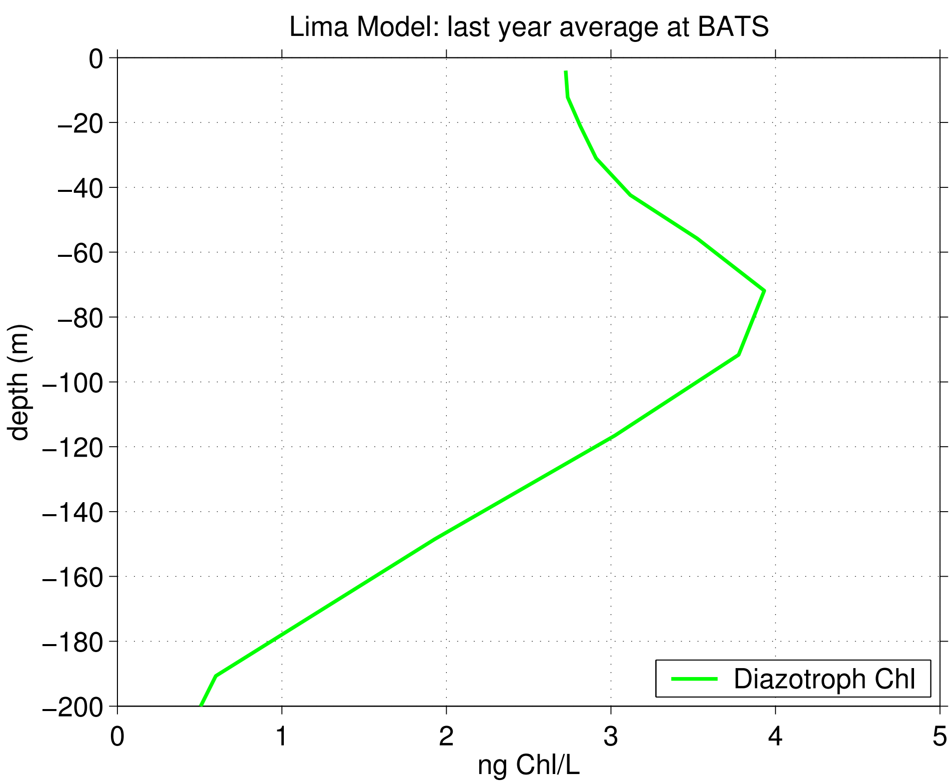

Fig. 6. Lima 3° run.

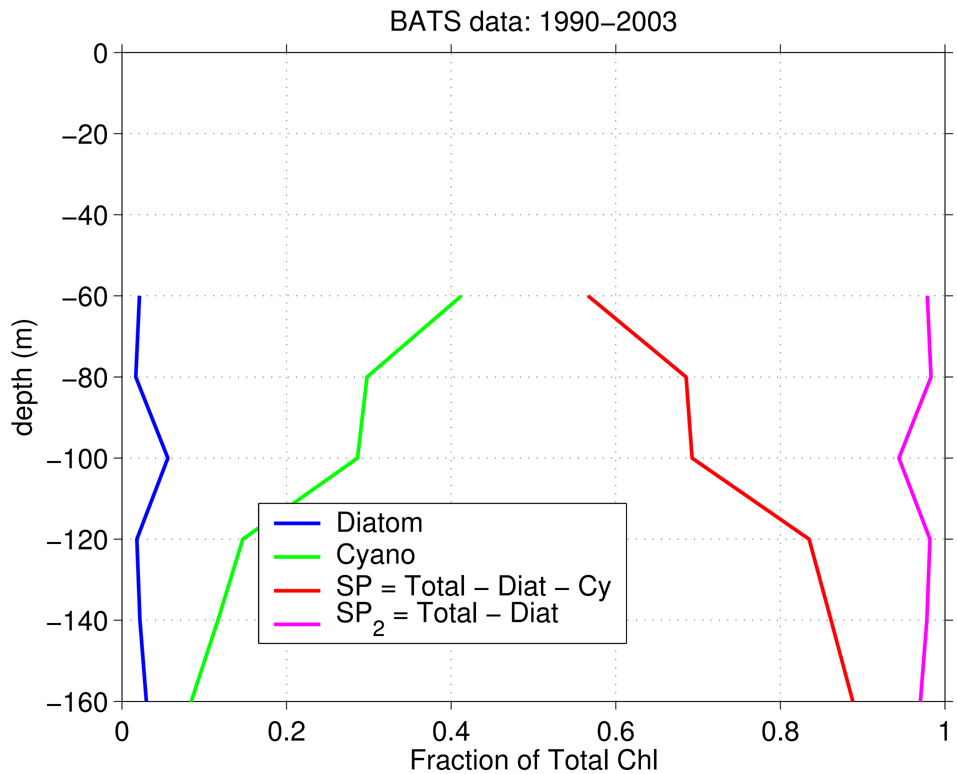

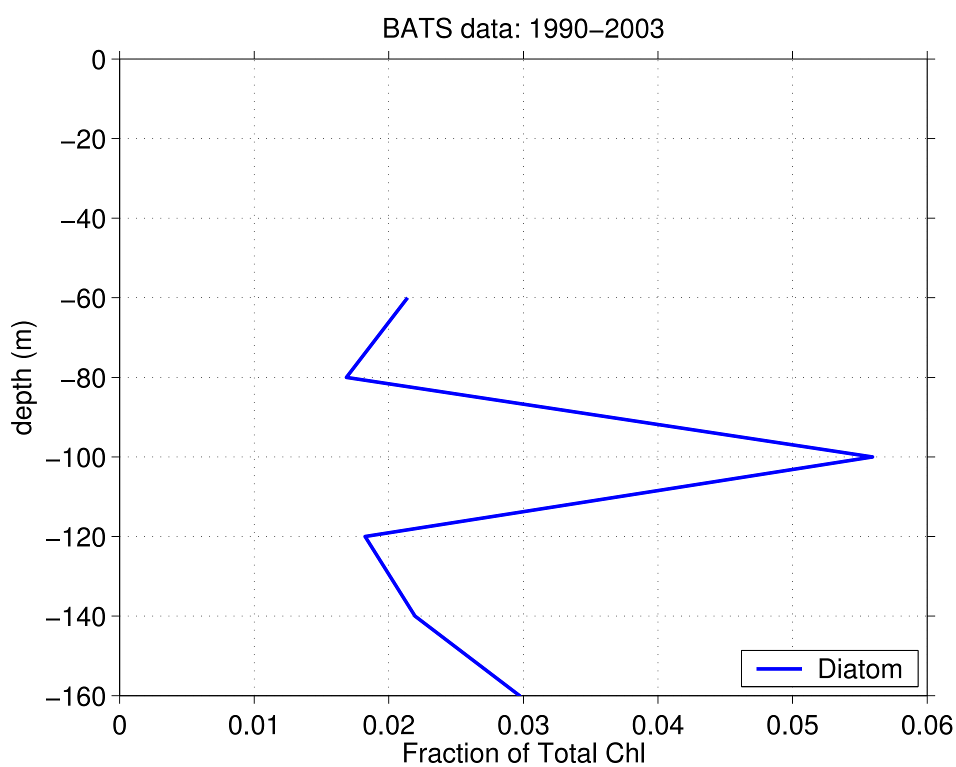

Fig. 7. BATS data.

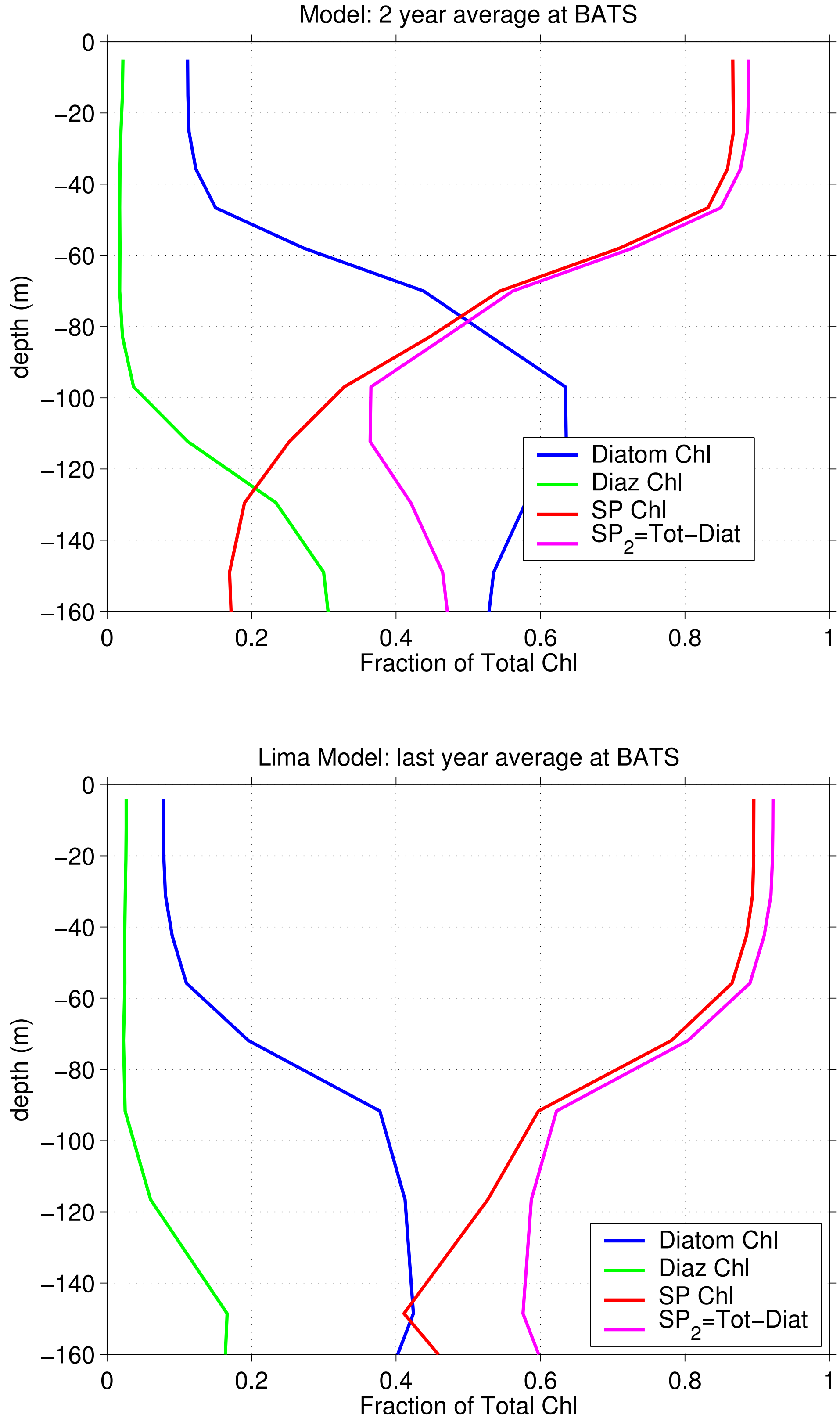

Fig. 8. (a) Maltrud 0.1° run. (b) Lima 3° run.

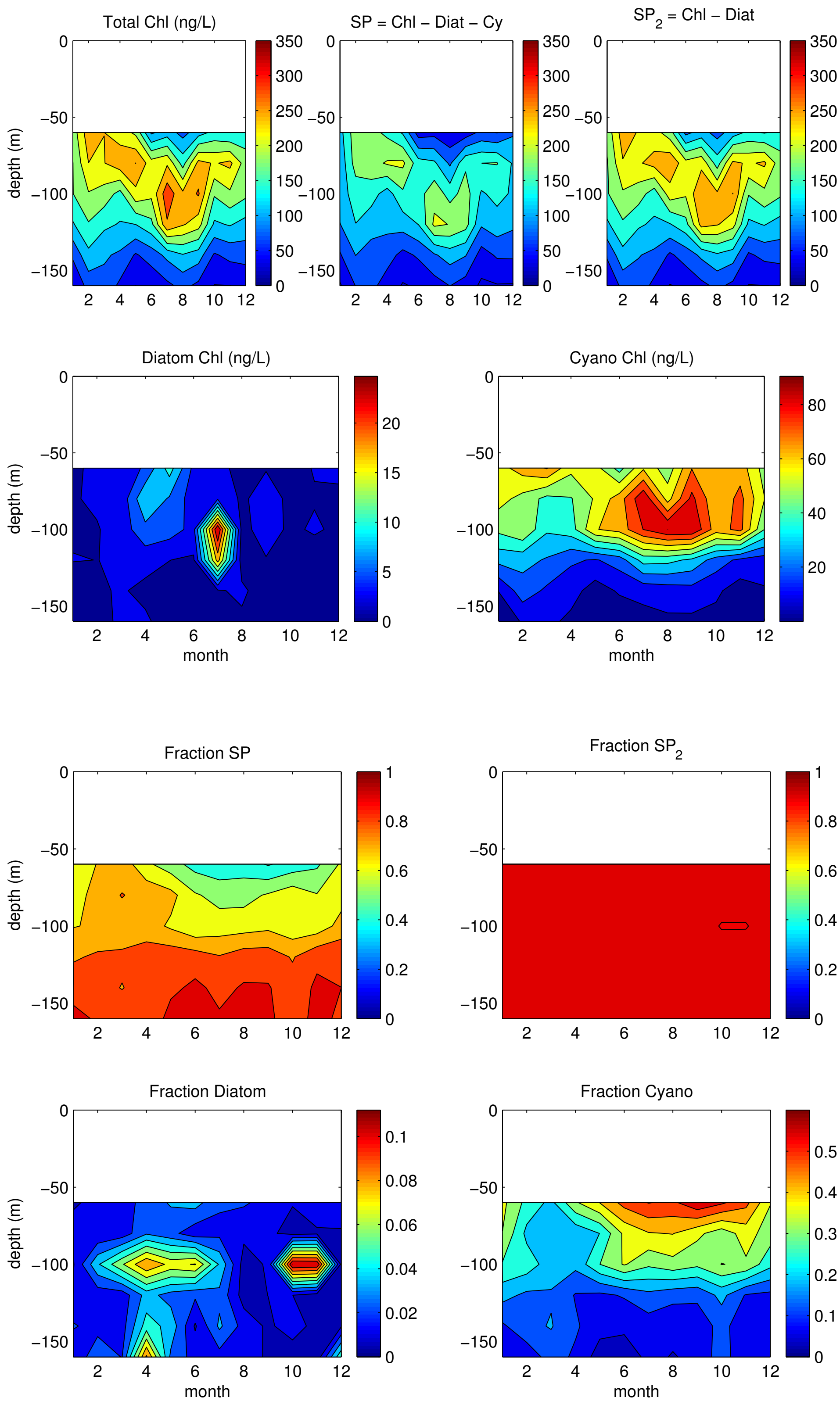

Fig. 9. 1990-2003 BATS data.

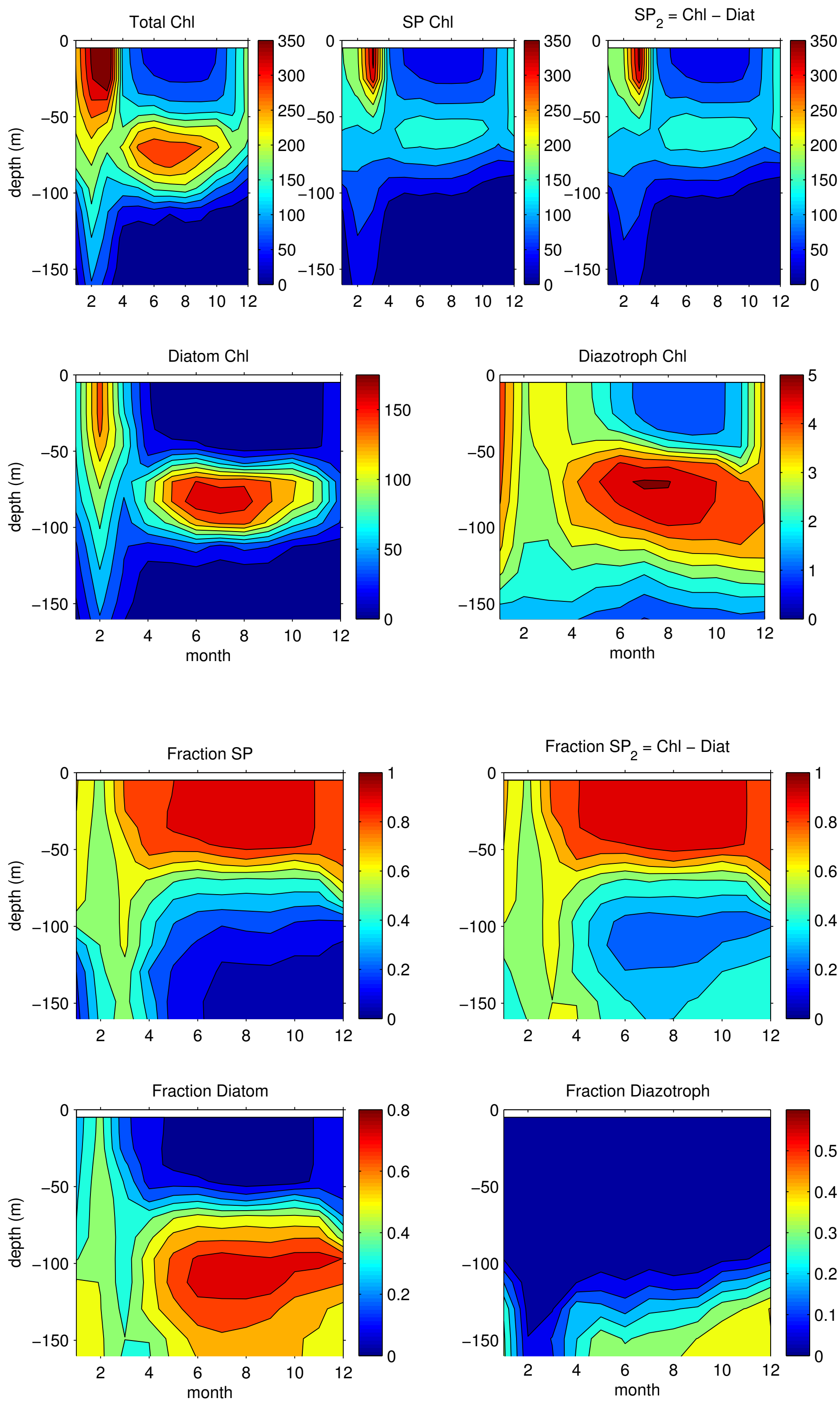

Fig. 10. Maltrud 0.1° run.

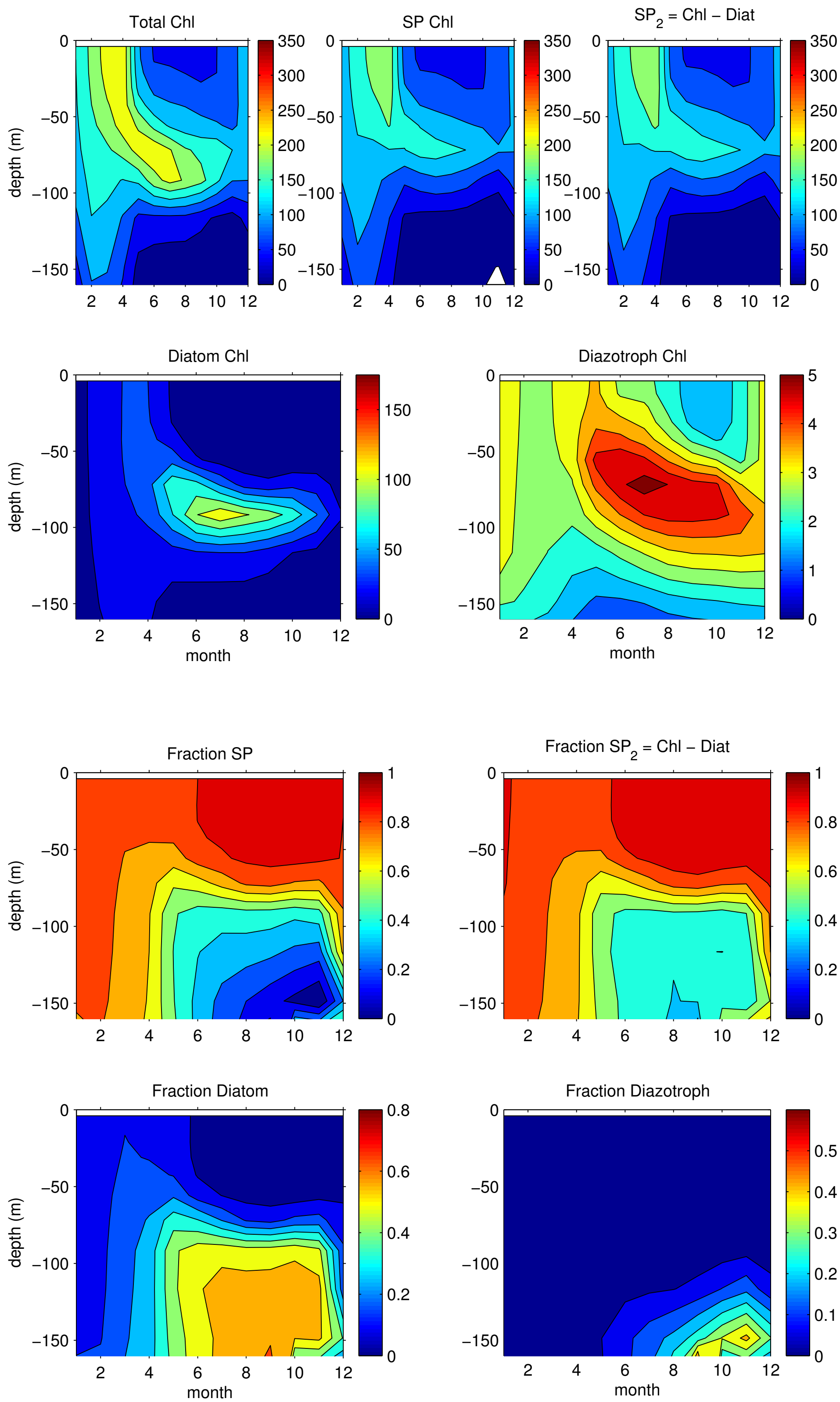

Fig. 11. Lima 3° run.

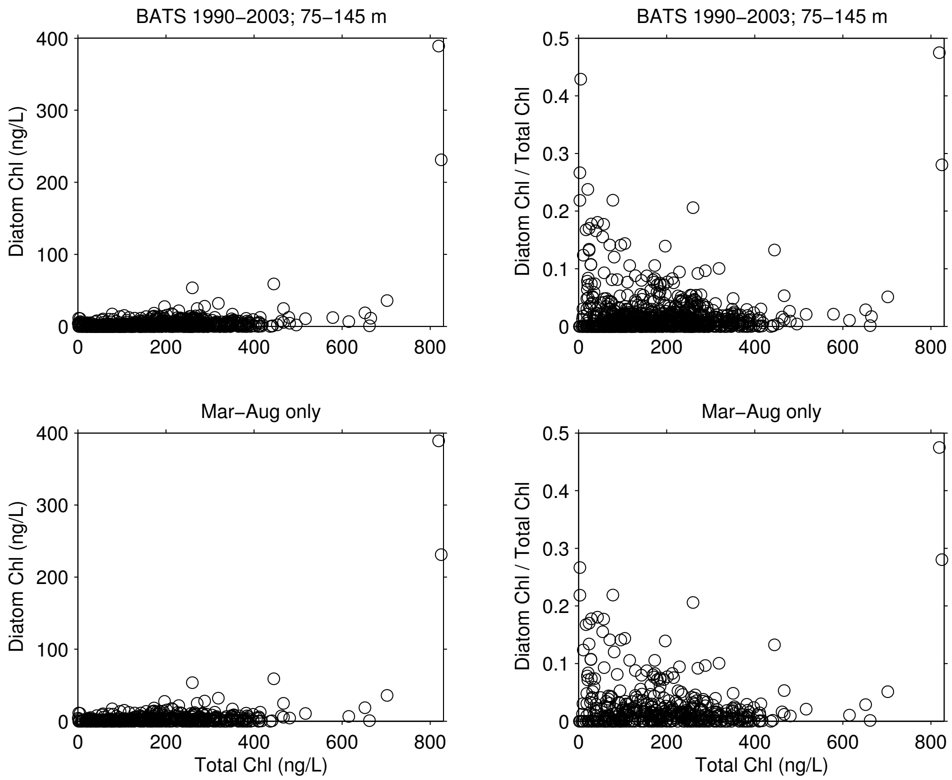

Fig. 12. BATS data.

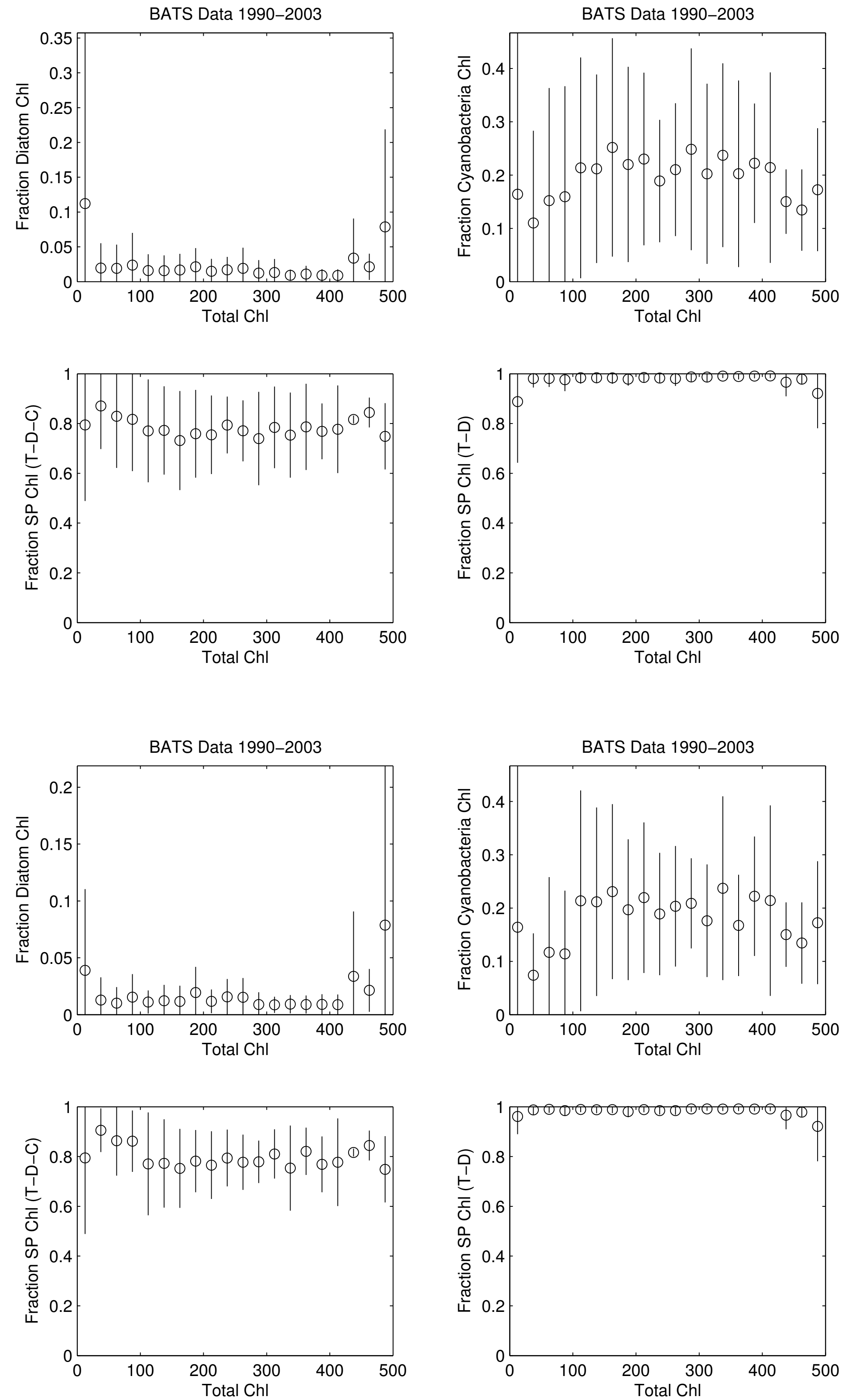

Fig. 13. (a) BATS data, 75-165 m. (b) As (a) with outliers > 3 std removed (iterated twice).

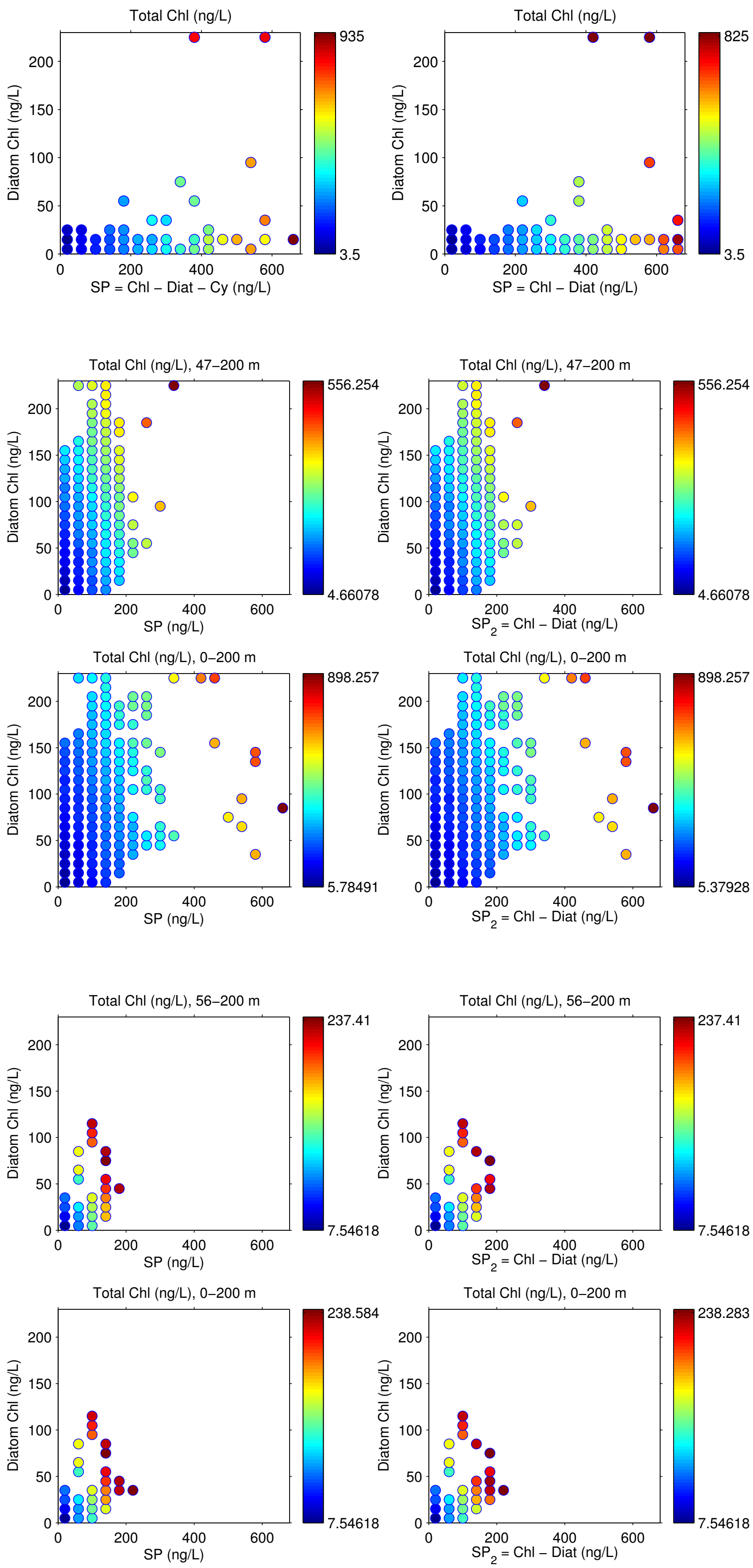

Fig. 14. (a) BATS data, (b) Maltrud 0.1° run, (c) Lima 3° run.

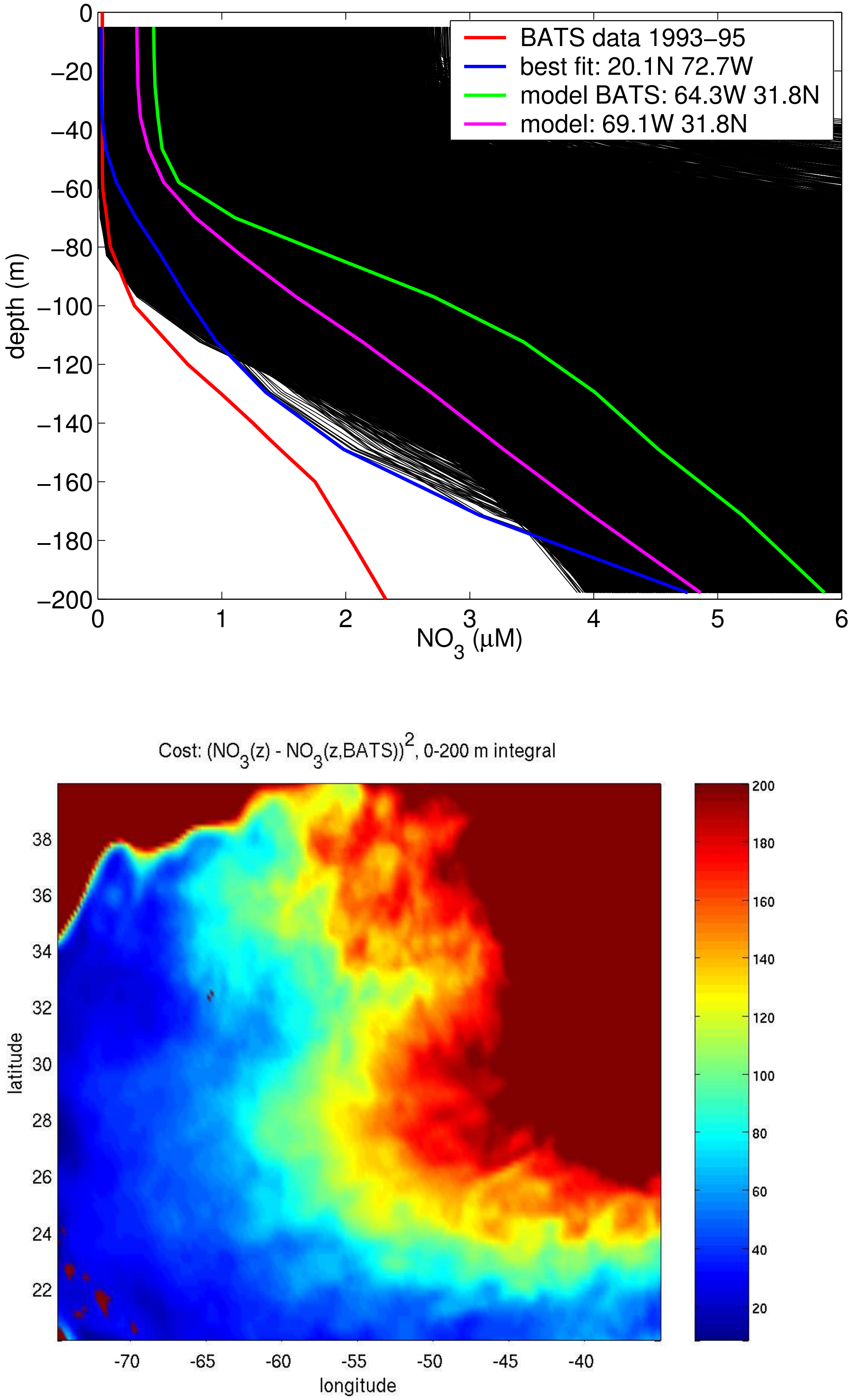

Fig. 15. 0.1° model.

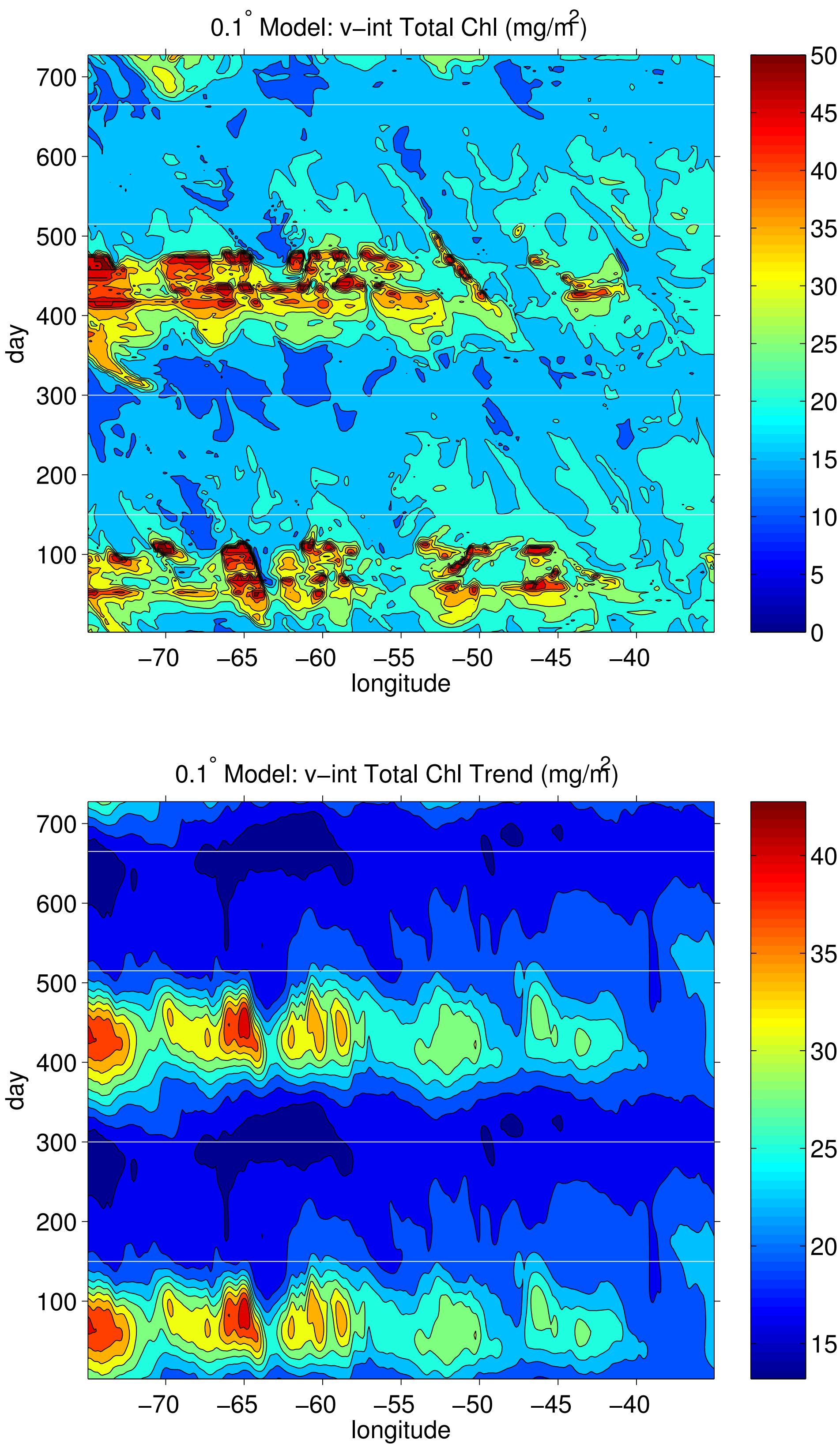

Fig. 16. 0.1° model. (a) original, (b) monthly trend.

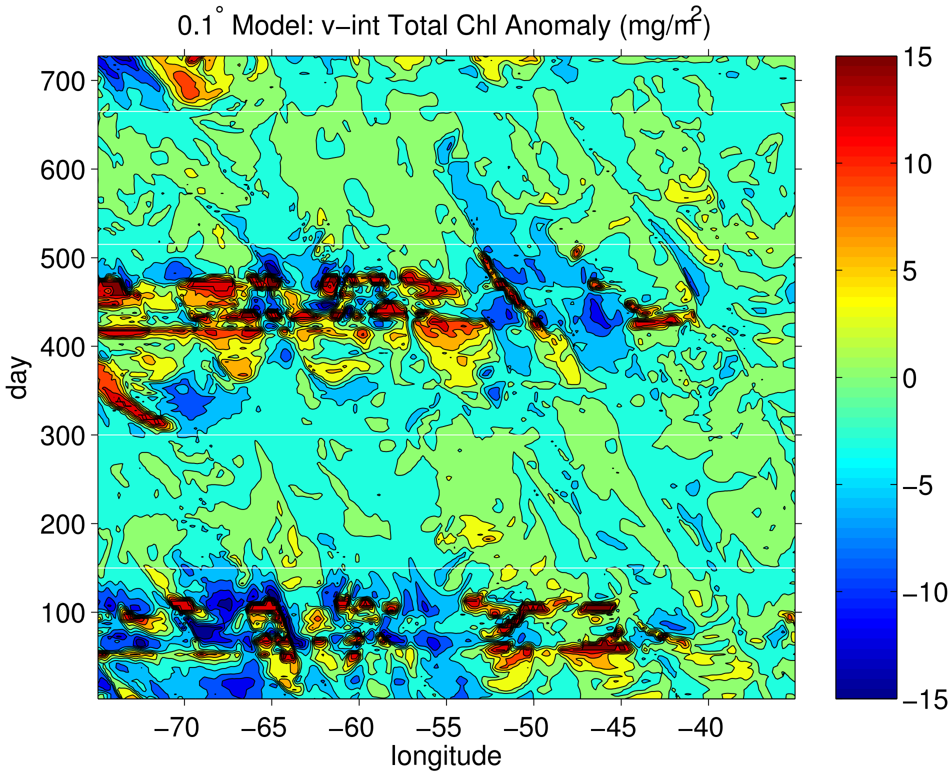

Fig. 17. 0.1° model. (a) eddy signal.